Separation Science and Technology
Publication details, including instructions for authors and subscription information:
http://www.informaworld.com/smpp/title~content=t713708471

Stabilizing Glass Bonded Waste Forms Containing Fission Products Separated from Spent Nuclear Fuel

Kenneth J. Bateman[a]; Charles W. Solbrig[a]
[a] C. W. Solbrig, Fuel Cycle Programs Division, Idaho National Laboratory, Idaho Falls, Idaho, USA

To cite this Article Bateman, Kenneth J. and Solbrig, Charles W.(2008) 'Stabilizing Glass Bonded Waste Forms Containing Fission Products Separated from Spent Nuclear Fuel', Separation Science and Technology, 43: 9, 2722 — 2746
To link to this Article: DOI: 10.1080/01496390802151831
URL: http://dx.doi.org/10.1080/01496390802151831

Separation Science and Technology, 43: 2722–2746, 2008

ISSN: 0149-6395 print/1520-5754 online
DOI: 10.1080/01496390802151831

Taylor & Francis
Taylor & Francis Group

Stabilizing Glass Bonded Waste Forms Containing Fission Products Separated from Spent Nuclear Fuel

Kenneth J. Bateman and Charles W. Solbrig
C. W. Solbrig, Fuel Cycle Programs Division, Idaho National Laboratory, Idaho Falls, Idaho, USA

Abstract: A model has been developed to represent the stresses developed when a molten, glass-bonded brittle cylinder (used to store nuclear material) is cooled from high temperature to working temperature. Large diameter solid cylinders are formed by heating glass or glass-bonded mixtures (mixed with nuclear waste) to high temperature (915°C). These cylinders must be cooled as the final step in preparing them for storage. Fast cooling time is desirable for production; however, if cooling is too fast, the cylinder can crack into many pieces. To demonstrate the capability of the model, cooling rate cracking data were obtained on small diameter (7.8 cm diameter) glass-only cylinders. The model and experimental data were combined to determine the critical cooling rate which separates the non-cracking stable glass region from the cracked, non-stable glass regime. Although the data have been obtained so far only on small glass-only cylinders, the data and model were used to extrapolate the critical-cooling rates for large diameter ceramic waste form (CWF) cylinders. The extrapolation estimates long term cooling requirements. While a 52-cm diameter cylinder (EBR-II-waste size) can be cooled to 100°C in 70 hours without cracking, a 181.5-cm diameter cylinder (LWR waste size) requires 35 days to cool to 100°C. These cooling times are long enough that verification of these estimates are required so additional experiments are planned on both glass only and CWF material.

Keywords: Casting, ceramics, electrorefining, fission products, nuclear waste, pyroprocessing, thermal stress

Received 8 January 2008; accepted 2 April 2008.
Address correspondence to C. W. Solbrig, Fuel Cycle Programs Division, Idaho National Laboratory, PO Box 1625, Idaho Falls, Idaho 83415-6180, USA. E-mail: charles.solbrig@inl.gov

INTRODUCTION

A major rate-limiting step in reprocessing spent nuclear fuel is the production of glass and glass-based waste forms (such as CWF), especially the final cool-down (1). The cooling rate can be enhanced with center-hole heat transfer and/or enhanced outer surface cooling (2). Rapid cooling is desirable for process efficiency, but has the potential to crack the consolidated product into many pieces due to thermal stress. Cracking of the waste form may not be desirable since it can cause handling difficulty and may change the leaching characteristics. Therefore, it is desirable to determine the optimum cool-down rate in order to form a more durable, stable product.

Storing unreprocessed spent nuclear fuel in a repository leaves a 100,000 year storage problem. Reprocessing spent fuel recovers useful fuel (Pu and other actinides) and depleted uranium, leaving only fission products. The fission products must then be converted to a form suitable for a storage time of 300 years, the approximate time it takes for radiation levels to decrease to that of natural uranium. Fission products are mixed with glass or glass-based mixtures, raised to a high temperature to melt and coalesce the components, and then solidified by cooling.

In the separation process which generated this research, the Argonne National Laboratory developed a method of pyroprocessing of spent metallic nuclear fuel (3). Useful fuel is separated from the waste (fission products) and depleted uranium in an electrorefiner. The fission products build up in the electrorefiner as chlorides in the LiCl-KCl salt electrolyte. When the concentration of fission products reaches a predetermined level, some of the fission-product-loaded salt is bled from the electrorefiner to be incorporated into a stable ceramic waste form (4). The separated fission product/salt mixture is then contacted with zeolite at 500°C in a V-mixer, where the salt is absorbed into the zeolite. This salt-loaded zeolite is then cold-mixed with borosilicate glass frit and consolidated into a CWF by heating to 915°C for a predetermined length of time, and then cooled. During the consolidation process, the zeolite converts into sodalite, forming a stable CWF product that is bonded together with the glass. The resulting form is suitable for long term storage in a facility such as Yucca Mountain.

The cooling process to be used in producing the CWF is the following:

1. cool quickly in the liquid region to a uniform temperature just above solidification,
2. cool slowly until solidification is complete because cooling at a very low rate during solidification eliminates the buildup of stress in the solid, and
3. then cool the solid at less than the critical-cooling rate to prevent cracking.

The data obtained in this work can be used to determine the critical-cooling rate in the solid region after solidification. Cooling in the solid region from a uniform temperature produces compressive stresses in the inner region and tensile stresses in the outer region.

An alternative method of cooling the CWF is to cool down in one process from the liquid region. Cooling from a high temperature in the liquid region at a high rate can cause the opposite stress condition upon reaching a uniform temperature than that observed here. That is, if the cylinder is able to endure the cooldown stresses, upon reaching room temperature, the inner portion of the cylinder can be in tension and the outer portion in compression. If this stress is greater than the tensile limit, it can cause a crack to originate from the center rather than the surface. If it is less, then the glass is considered tempered and can withstand tensile loads that non-tempered glass cannot. The faster the cooling rate, the higher the center tensile stress. The magnitude of this stress is determined by the rate of cooling within the transformation range of temperatures, the coefficient of expansion, and the size. When the glass is homogeneous, the stresses and strains can be reduced to a low value by cooling it gradually (5). This cooling process is not analyzed in this work.

The model developed here represents the stresses developed when a glass-bonded brittle cylinder (used to store nuclear material) is cooled from high temperature (but below the solidification temperature) to a temperature at which it can be handled ($\sim 100^{\circ}C$). The stress is then used to determine the critical-cooling rate, the rate which separates the cracking regime from the non-cracking cooling rates. Experimental data are obtained on small borosilicate glass cylinders to determine the empirical parameters needed to apply this model to glass. Experiments with borosilicate glass were used with our model because its properties are known with more certitude than ceramic waste. It is expected that this model can be used to extrapolate to other materials, such as CWF, and larger cylinder sizes and that additional data will be needed to verify or modify the extrapolated numbers. The model points to the ratio of the coefficient of thermal expansion (CTE) to the tensile stress limit as being the most important parameter, with specific heat, density, thermal conductivity, and Young's modulus being secondary parameters.

As will be seen, the model is consistent with the data obtained and allows the data to be represented. The model predicts that the critical-cooling rate decreases with the cylinder radius squared and implies that long cooling times are required for large cylinders to prevent cracking. If this conclusion is correct, and if the conclusion extends to waste forms such as CWF, the rate limitation will affect the design of reprocessing plants which produce waste forms 6 feet in diameter, as in a 100 metric tonnes of heavy metal (MTHM) per year plant (3). This

plant size represents that needed to service a single nuclear 2000 MW power-generating plant site (6). Plant sizes of 2000 MTHM/year or more would be needed if nationwide processing plants are used (7).

O'Holleran, (8) provides justification for believing that CWF and glass will exhibit similar behavior in failure. On p. 219, (8) reports no statistical differences exist between glass and zeolite ratios of 1 to 1 and 1 to 3 and concludes that glass is the binder which penetrates the zeolite, producing similar microstructure between the different concentrations. On p. 220, (8) discusses the similarity of properties of the CWF to various glasses. In private communication, O'Holleran indicates that the mechanical and thermal properties of CWF are related to glass because the glass is holding the material together. Also, the CTE would be similar because the glass is the framework of the CWF.

Stress in brittle materials has been discussed in several publications. Timoshenko (9) derives a stress equation due to general thermal gradients in the normal direction in flat plates (p. 436, Eq. f), a formulation which is equivalent to that presented here. He further presents results for solid circular cylinders. The circumferential stress (Eq. 250) is similar to that in flat plates, and the axial stress (Eq. 253) is the same. Jaeger (10) presents stress calculations based on analytical solutions for temperature profiles of the type presented in the next section, inserted into the Timoshenko circumferential stress equations. Hasselman (11) used the analytical results of (10) to obtain an approximate linear relationship between the inverse of the Nusselt number and the inverse of the maximum calculated stress (Equation 6, 11). From this, he determines the maximum initial temperature from which a specimen can be cooled with a given heat-transfer coefficient. In the work presented here, the inverse is presented. That is, given an initial temperature, the maximum cooling rate is determined which will prevent cracking. Experimental work is also reported on in the literature (for example, in 12, 13, and 14), but integration of such material into this work is beyond the scope of this paper and awaits a further study.

The outline of this paper consists of the following: the analytical model is described in Section II. Cooling-rate cracking and non-cracking data obtained on small-diameter (7.8 cm diameter) glass-only cylinders are discussed in two sections: the experimental procedure in Section III and the test results in Section IV. In Section V, the model and experimental data are combined to determine the critical-cooling rate which separates the non-cracking, stable-glass region from the cracked, non-stable glass regime. In Section VI, the model is then used to extrapolate the minimum cooling times required to keep large-diameter cylinders from cracking. These glass results represent Phase I of a continuing study. We intend to verify/modify the analysis if warranted when experiments are run on larger diameter cylinders and other materials such as CWF.

ANALYTICAL MODEL

For efficacy, cool-down of a cylinder was modeled with constant properties using a consolidated density, ρ, of 2.15 gm/cc, specific heat, C_p, of 1401 J/kg°C, and thermal conductivity, k, of 1.71 W/(m°C). Use of these constant properties allows the solutions to be applied readily to multiple conditions (15) presents an analytical solution to this problem for an infinite heat-transfer coefficient and compares well to the solution here.

The initial condition for the temperature of the cylinder at cool-down is T_{init} (525°C to 675°C), and T_{surr} is the surrounding temperature for all surfaces (25°C for cool-down). The independent variables are the radial coordinate, (r), the axial coordinate, (z), and time, (t). The conduction equation for constant properties in a cylinder is:

$$\rho C_p \frac{\partial T}{\partial t} = k \frac{1}{r} \left(\frac{\partial}{\partial r} r \frac{\partial T}{\partial r} \right) + k \frac{\partial^2 T}{\partial z^2} \tag{1}$$

This equation is written in dimensionless form, where the dimensionless temperature T' is defined as

$$T' = \frac{T - T_{surr}}{T_{init} - T_{surr}} \tag{2}$$

The conduction equation can then be written as:

$$\frac{1}{\alpha} \frac{\partial T'}{\partial t} = \frac{1}{R^2} \frac{1}{r'} \left(\frac{\partial}{\partial r'} r' \frac{\partial T'}{\partial r'} \right) + \frac{1}{L^2} \frac{\partial^2 T'}{\partial z'^2} \tag{3}$$

where $\alpha = k/\rho C_p$ $r' = r/R$ *and* $z' = z/L$

The value of α for the physical properties specified above is 20.4 cm^2/hr. Multiplying through by R^2 yields

$$\frac{\partial T'}{\partial t'} = \frac{1}{r'} \left(\frac{\partial}{\partial r'} r' \frac{\partial T'}{\partial r'} \right) + \frac{R^2}{L^2} \frac{\partial^2 T'}{\partial z'^2} \tag{4}$$

where $t' = t\alpha/R^2$ *and* R/L *are the two independent parameters.*

An effective convection coefficient for heat transfer, h, (that is, linear heat loss) is used in this model, and radiation heat transfer is approximated in this effective coefficient when h is determined from the experimental data. This assumption simplifies the data analysis and also allows similarity analysis to be used. For a finite heat-transfer coefficient, h, (which is assumed constant) the boundary condition at r = R is

$$k \frac{\partial T}{\partial r} = -h(T - T_{surr}) \tag{5}$$

Or in dimensionless terms, this boundary condition becomes

$$\frac{\partial T'}{\partial r'} = -\frac{hR}{k}T' = -\frac{1}{2}\frac{hD}{k}T' \tag{6}$$

where hD/k is the Nusselt number, an additional independent parameter.

The boundary condition at r = 0 is zero heat transfer due to symmetry. This condition specifies a zero radial temperature derivative in both the dimensional and dimensionless forms and introduces no new dimensionless quantities.

A similar axial-boundary condition was assumed for the heat transfer, but r was replaced with z in the top surface, and a positive sign replaced the negative one on the bottom surface. The heat-transfer coefficient used for the end boundaries was assumed to be the same as that used around the circumference. A similar parameter, hL/k, is obtained from the end boundary conditions, but it is not independent since it is composed of the two parameters hR/k and L/R.

The thermal stress in the cylinder is generated by the temperature gradient within the cylinder. Each surface in the cylinder, defined by r = "a constant," is at a unique temperature, and each has a different stress-free length, both circumferentially and longitudinally, corresponding to that temperature. Since the planes were all intrinsically attached, the overall circumference and length of the surface was determined by the average temperature of the plate. The stresses were calculated by assuming that each surface was forced to be the same length as the average, making them directly related to the average temperature. As discussed later, the interior stress is slightly different in the circumferential direction but identical on the surface. The surfaces that were at a higher temperature than the average temperature were, therefore, under compression, and the planes that were at a lower temperature were in tension. In the longitudinal direction, the amount that surface i must be elongated to reach the overall length, ΔL_i, is:

$$\Delta L_i = L\alpha_T(T_{avg} - T_i) \tag{7}$$

where L = length of the plate determined by the average temperature
α_T = coefficient of thermal expansion
T_i = temperature of surface i
T_{avg} = spatial averaged temperature of plate

The tensile stress that is induced in a plane elongated by the length ΔL_i is approximately

$$\sigma_i = \frac{E}{1-\mu}\frac{\Delta L_i}{L} \tag{8}$$

where E = Young's modulus
μ = Poisson's ratio

Substituting for ΔL_i yields the thermal stress, σ, at any surface, i, as

$$\sigma_i = \frac{E\alpha_T}{1-\mu}(T_{avg} - T_i) \tag{9}$$

so the thermal tensile stress, $\sigma_{\max}$, on the surface (which is the radial maximum) can be calculated by

$$\sigma_{\max} = \frac{E\alpha_T}{1-\mu}(T_{avg} - T_{surr}) \tag{10}$$

where T_{avg} = average temperature of the cylinder
T_{surr} = surface temperature.

This agrees with Equation 253 of (Ref. 9). A similar equation is obtained for the surface stress in the circumferential direction. The circumferential tensile stress is greater than the longitudinal stress for r' less than 1 but is identical on the surface (Equation 250 of Ref. 9). The surface stress is still the radial maximum. Therefore Equation 10 represents the maximum tensile stress in both the longitudinal and circumferential directions.

The dimensionless surface stress, $\sigma_{\max}$, can then be defined as

$$\underline{\sigma}_{\max} \equiv \frac{\sigma_{\max}(1-\mu)}{E\alpha_T(T_{init} - T_{surr})} = (T'_{avg} - T'_{\max}) \tag{11}$$

which is the dimensionless stress in both the longitudinal and circumferential direction.

The reference EBR-II CWF has a diameter of 52 cm and a consolidated length of 300 cm. This equates to a length to diameter ratio of approximately 5.8. The experiments were conducted on cylinders with length to diameter ratios of 1 or less. This makes the experimental results conservative with respect to the EBR-II-CWF size since the smaller length-to-diameter ratios in the tests added larger longitudinal stresses.

EXPERIMENTAL METHODS

Glass cylinders were formed with borosilicate glass frit and then tested for resistance to damage at various cooling rates. They were formed by first loading the frit into stainless steel canisters (D = 8.4 cm, L = 10.4 cm, V = ~600 cc), tamping, inserting the canisters in a furnace, heating to an elevated temperature, holding at that temperature for three hours, then cooling in the furnace at a slow rate. The frit had an initial tamped density of approximately 1.26 g/cc and coalesced to about 2.1 g/cc in the consolidation process. The canisters were coated on the

inside with boron nitride to reduce sticking to the container after consolidation. The most successful were formed by heating the canister to 670°C at 10°C/min, holding for 3 hours, and then cooling in a closed furnace (5°C/min), usually overnight. The 670°C temperature is above the glass-softening temperature which allowed the glass frit to coalesce. The three-hour hold time was estimated by determining the time it would take to bring the centerline of the cylinder to 99% of hold temperature, using the above equations in a heat-up mode, along with approximate thermal properties for glass frit. The slow cool-down rate ensured there were no residual stressed in the glass.

The coalesced glass cylinders often looked frosty on the outside, but glassy in the middle when broken open. Most pulled away from the container wall when turned upside down and were removed with no, or minor, coaxing. Cylinders without a metal or other ceramic shell attached were desired in order to observe the fracture characteristics of the failed cylinders. The condensed height of the cylinder was about 7.4 cm, although the top surface often sloped a small amount. The diameter of a typical cylinder at the top was 7.36 cm at the top, 7.70 cm at the middle, and 8.26 cm at the bottom. The increase in diameter from top to bottom shows that the cylinders slumped a small amount, a fact that was responsible for the inability to remove some of the cylinders from the beakers when higher hold temperatures were used.

The formed cylinders were then used in cool-down experiments to test whether they would crack under various cool-down rates. The tests were conducted by raising the temperature of the cylinders at 10°C/min from ambient to a pre-determined hold temperature and holding for two hours. When compared to the hold time used to form the glass frit, less hold time was required to bring the center temperature of the consolidated cylinders up to temperature. This is because the consolidated material had a higher conductivity and thermal diffusivity than unconsolidated. The heat-up rate of 10°C/min was selected based upon previous experiments when faster rates caused the cylinders to fail during heat up. Heatup failure of the glass cylinder was not of interest because when CWF is processed, heat up will affect the non-coalesced material and cracking will not be an issue. Most of the hold temperatures were in the range of 575°C to 625°C, although some were outside of this range. Above this range, the glass becomes spongy and can flow slowly. A range of cooling rates were obtained by cooling the cylinders

1. in the closed furnace,
2. in an open furnace,
3. outside the furnace by natural circulation,
4. with fan cooling at low speed,

Figure 1. Results of test 32 which shows the cylinder unchanged.

5. at medium speed, or
6. at high speed.

Three representative examples of cylinders which were subjected to cooling tests are shown in the Figs. 1 through 3, in order from no damage to significant damage. Figure 1 shows the cylinder from Test 32 which was heated to 625°C, but cooled at a slow rate so it had very low thermal stresses and showed no cracking or damage. This cylinder was almost unchanged by the test except for a slight indent seen on the top of the cylinder. This was caused by the dilatometer rod in contact with the cylinder during the test. As the temperature increased and the cylinder became soft, it could no longer push the dilatometer rod up as it expanded. The indentation remained upon solidification.

Figure 2 shows the cylinder from Test 40. It was heated to a lower hold temperature (575°C), but was subjected to a higher cooling rate, causing mild thermal stresses that cracked the cylinder into four pieces. This fracturing appears to be close to the critical cooling rate boundary between facture and non-fracture. The surface area increased by somewhat more than a factor of 2.

Figure 3 shows the cylinder condition after Test 33. During this experiment, the cylinder broke into a number of pieces, which scattered

Figure 2. Resulting fractured cylinder from test 40 C.

over the experimental pad due to the high thermal stresses imparted in the cool-down. When that happened, the thermocouple no longer maintained contact with the broken cylinder and no longer measured the

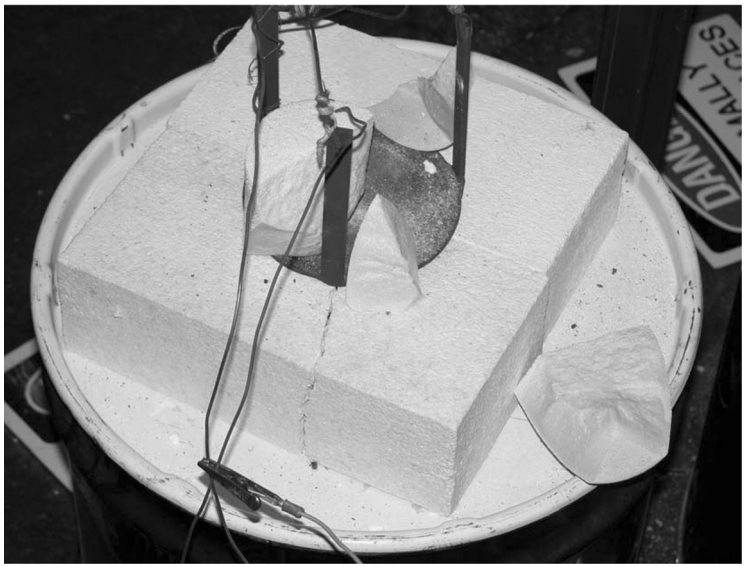

Figure 3. Resulting broken cylinder from test 33D.

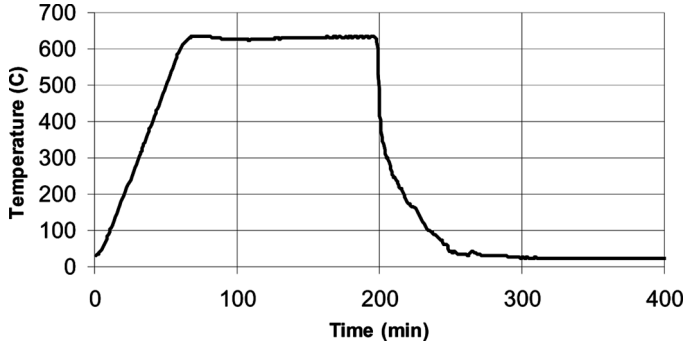

Figure 4. Heat-up and cool-down of thermocouple T4 during test 33.

surface temperature. The broken pieces in Figure 3 are shown in the position they reached after the cylinder broke apart. In addition, the larger pieces easily broke into smaller pieces.

Figure 4 shows the temperature profile of Test 33. The temperature plotted is that of thermocouple T4, which was positioned so that the end was touching the side surface at mid-height. A second thermocouple (not plotted on the figure) was pressed onto the top surface. When it was in good contact, it agreed with the thermocouple on the side, indicating the temperature was nearly uniform over the surface as it cooled down. Attempts to insert thermocouples in the glass resulted in a defective cylinder, so only pressed-on thermocouples were used.

The temperature profile shows the three regimes in the experiment: heat-up, hold, and cool-down. The initial heat-up was at 10°C/min, and thermal equilibrium between the furnace and surface was achieved at the hold temperature of 632°C in about an hour. The temperature overshot a bit (by 10°C) due to the PID controller. By the end of a 2-hour hold, the temperature had settled in at roughly 632°C. Approximately 200 minutes into the run, the furnace was uncovered, and the cylinder was removed from the furnace and placed on a firebrick pad. It then cooled by free convection in ambient air.

At approximately 27 minutes into cool-down, the cylinder fractured, scattering pieces up to 2 feet away. The scattering of the pieces is evidence of cracking due to tension on the surface and in the outer region of the cylinder. The air conditioning in the room was on, which may have enhanced the rate of cooling. At the time of destruction, the surface temperature was close to room temperature, and the loss of thermocouple contact with the surface is not noticeable on the plot.

The thermocouple (TC) was attached to the holder, and the TC junction was forced to contact cylinder surface by pressure. When the cylinder was removed from the furnace, the thermocouple often became detached from the surface. The temperature profile during this period can be estimated from the profile after it was reattached. Smoothing of this temperature profile has been done in plotting the cool-down portion of the profile in Fig. 4. The error in measuring the cooling rate was always in the direction of overestimation. This is because the thermocouple was merely pressed onto the cylinder, so any contact resistance or change in contact pressure would produce a lower reading than the actual surface temperature.

EXPERIMENTAL RESULTS

The test matrix and results are shown in Table 1. The successful tests, identification numbers, and results (damage or no damage) are shown. Identification numbers can be used to determine the correspondence between the pictures, the test results in Table 1, and the temperature profiles presented in later figures. Enough tests were run at each temperature to bound the critical cooling rate at that temperature. Bolded values indicate test specimens that experienced no damage, and non-bolded indicate those that experienced damage. The bolded, non-bolded fonts indicate a division between failure and non-failure of the cylinders. It can be seen that at high hold temperatures, low cooling rates cracked or broke apart a cylinder. Conversely, at low-hold temperatures, a higher cooling rate was required to crack or break apart a cylinder. Additionally, two distinct damage levels were noted. Cylinders exposed to mild thermal stresses cracked into two to four pieces and are labeled with a "C" for cracked (see Test 40 shown in Fig. 2). Cylinders with high thermal stresses broke into many pieces and were labeled with a "D" for damaged (see Test 33 as shown in Fig. 3). The distinction between these damage levels is made to show tests which significantly exceed the critical cooling rate (D) and those that should be close to it (C).

Most of the tests were run with hold temperatures less than the consolidation temperature. The reason for this was that stresses cannot build up until the cylinder becomes solid. The theory of Section II applies strictly to solid cylinders of constant physical properties, especially density. However, if the cylinders are cooled slowly while solidifying, significant stresses do not build up during solidification. For this reason, two of the high-temperature consolidation tests (Tests 20 and 27) were included in the table. They showed no damage when the cylinders cooled from 670°C at a low cooling rate. Data from a dilatometer used to measure

Table 1. Summary of solid cylinder test results

Cooling condition	Cooling rate	Approximate 2 hour hold temperature, (°C)					
	°C/min	525	575	600	625	675	725
Furnace (covered)	5					**20ok,27ok**	
Furnace (open)	15 to 50			**44ok+**	**32ok+**		
On Table (free conv.)	80 to 160	**13ok***	**19ok**+**	42C+	33 D+		11D no hold
Low Speed fan	50 to 240		37C,40C+	22 D+			
Med Speed fan	100		46C+				
High Speed fan	350		16 D+				

ok = undamaged in cool-down.
*Visible cracks, cracking sounds, stayed one piece.
C = cracked; ~4 pieces.
**Broke on heat-up during the next test.
D = Destroyed; many pieces.
+Data considered valid and stress evaluated.

cylinder height during some of the tests indicated that the cylinders were completely solidified below 625°C.

Hold temperature and the cooldown rate are the main parameters in determining the possible thermal stresses in the cylinder. Surface temperature histories for six of the experiments are included in Fig. 5. Only the cool-down portions of the experiments are shown. The test number, the physical result of the experiment, the hold temperature, and the method of cooling are indicated on each of the plots.

This figure shows that damage to the cylinders was caused by higher cooling rates. The higher the rate, the more severe the cracking. Cooling rates less than that experienced in Test 19 provide a safe region for cool-down. The cooling rate in Test 19 is close to the critical-cooling rate, which is defined as the rate at which the boundary between damaged and non-damaged cylinders exists. The hold temperature is also important, but it is not clear from this figure how this interacts with the cooling rate. In fact, the cooling rate for Tests 19 and 33 appear similar, but Test 33 broke apart with force while Test 19 exhibited no damage. The higher hold temperature of 33 (632°C) compared to 19 (580°C) is responsible for

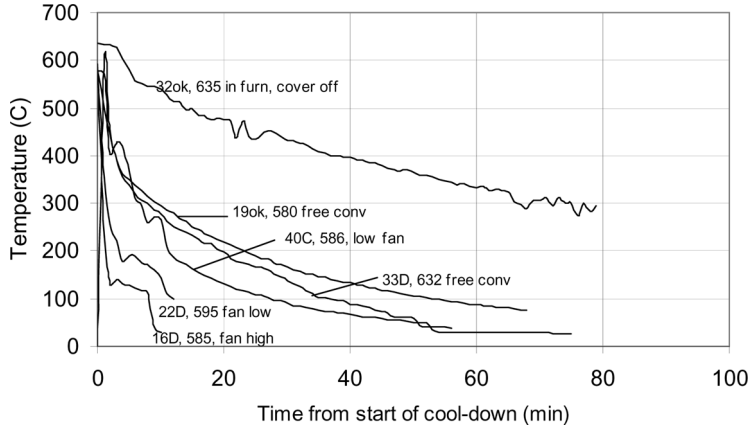

Figure 5. The cool-down portion of several experiments.

the difference. Application of the analytical model clears up these effects as described next. It shows that the maximum stress developed in the transient determines failure. So high temperatures and low cooling rates can cause failure as can low initial temperatures and high cooling rates so long as the developed stress exceeds the limit.

ANALYSIS OF EXPERIMENTS

The analytical model presented earlier was used to generate the predicted cooling-rate curves, which are used with the experimental data to estimate the effective heat-transfer coefficients in each test. The calculations were made for a range of effective heat-transfer coefficients which covered the cooling-rate range of interest. Five calculated reference plots of surface cooling rates for the experiment size with an initial hold temperature of 630°C are plotted in Fig. 6. The surface-cooling data from two experiments are also included. Since Test 32 did not fail and Test 33 did, the reference plots include regions on either side of the boundary between the cooling-rate stress damage/non-damage regions.

The tensile surface stresses that correspond to the cooling rates in Fig. 6 are shown in Fig. 7 and verify that the desired stress range is covered. The maximum stress exceeds 10,000 psi, which is the limiting tensile stress of glass (16). The thermal stress during the cool-down period, calculated as a function of radius from the equations in Section II, shows that the inner region is in compression and the outer is in tension. Only the outer surface and center plane stresses are shown in Fig. 7 because these are the largest and were calculated assuming a CTE of 9×10^{-6}

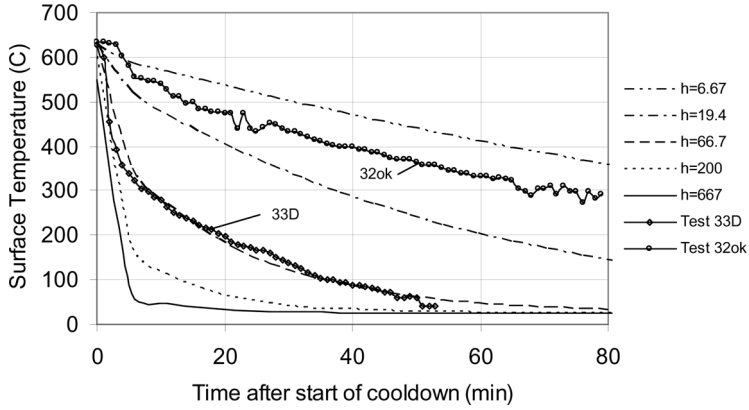

Figure 6. Cool-down rates from the analytical model and two experiments.

cm/cm°C, a Young's modulus of $10 \times 10^{+6}$ psi, and a Poisson's ratio of 0.16. The 10,000 psi damage tensile-stress limit for glass is seen to be broached at the three highest cool-down rates. The compression stresses in the center of the cylinder are a bit larger, but the compression stress limit is over a factor of 10 higher (> 200,000 psi), so compression fracture is of no concern compared to tensile fracture.

The experimental surface temperatures drop off faster than the calculated values, indicating the heat-transfer coefficient varies in the experiment whereas it was assumed constant in the analysis. Experimentally, it is greater during the early part of cooling and less later due to the power-law effect of thermal radiation on the heat-transfer coefficient. The heat-transfer coefficient as a function of time cannot be calculated directly from the surface temperatures data because, as Equation 5 indicates, both the temperature and the radial-temperature gradient would be necessary for this. It could be calculated by imposing the measured temperature-time profile on the model, but this can cause numerical instability to occur due to measurement-error oscillations. Use of an approximately constant h circumvents this problem.

A deficiency of the analysis is noted in the time of failure. The calculated maximum stress occurs approximately 10 minutes after the start of cooling, so that one would expect failure at this time. The experiments indicated it often occurred later, as much as forty minutes after start of cool-down.

The CTE is estimated to be an average over the temperature range for the Pyrex (borosilicate) glass tested in these experiments. Pyrex has literature-quoted values of 3.6×10^{-6} cm/(cm·°C) in the temperature range of 21°C to 471°C and a value of 15.1 $\times 10^{-6}$ cm/(cm·°C) in the

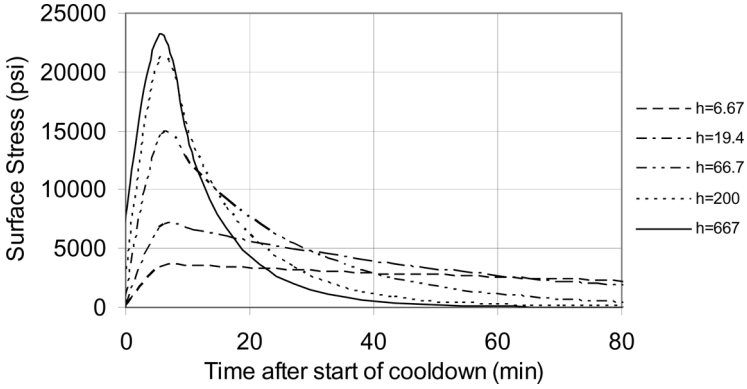

Figure 7. Surface stresses calculated from the previous cool-down rates.

range 552°C to 571°C (17). Measurements made in this study with a dilatometer (but not reported here due to lack of accuracy of the method) showed that CTE increases with temperature and the average value to be in the vicinity of 9×10^{-6} cm/(cm·°C) in agreement with the above literature values. The surface stresses shown in Fig. 7 are the same for both the circumferential and longitudinal stresses (9). Since these stresses are perpendicular to each other, they would combine on a 45 degree plane between the two to produce a stress $\sqrt{2}$ greater than the value plotted.

The two experiments plotted in Fig. 6 had hold temperatures close to 630°C; Test 32 with an initial temperature of 635°C and Test 33 with an initial temperature of 632°C. These can, therefore, be analyzed with the reference plots of Figs. 6 and 7. A heat-transfer coefficient can be obtained by comparing the experimental data to the calculated values in Fig. 6. This h-value can then be used to obtain the stress from Fig. 7. For example, in Fig. 6, the experimental data from Test 32 falls between the lines for $h = 6.67$ W/(m^2·°C) and $h = 19.4$ W/(m^2·°C). An interpolation would correspond to a computed h of roughly 8.7 W/(m^2·°C). Applying this value to Fig. 7 yields a maximum surface stress of about 5,000 psi. Similarly, Test 33 corresponds to a computed h of about 58 W/(m^2·°C), which yields a maximum surface stress of about 15,000 psi. Multiplying by 1.41 yields maximum stresses of 7,070 psi and 21,200 psi, respectively, indicating that, in agreement with the experiment, the cylinder from test 32 should not have been damaged while that from 33 may have been. The powerful failure of Test 33 signifies the tensile stress limit may be close to the quoted 10,000 psi.

In order to analyze other experiments with different initial temperatures, the same type of charts would have to be produced for each initial temperature and diameter of cylinder. A simpler method is to produce

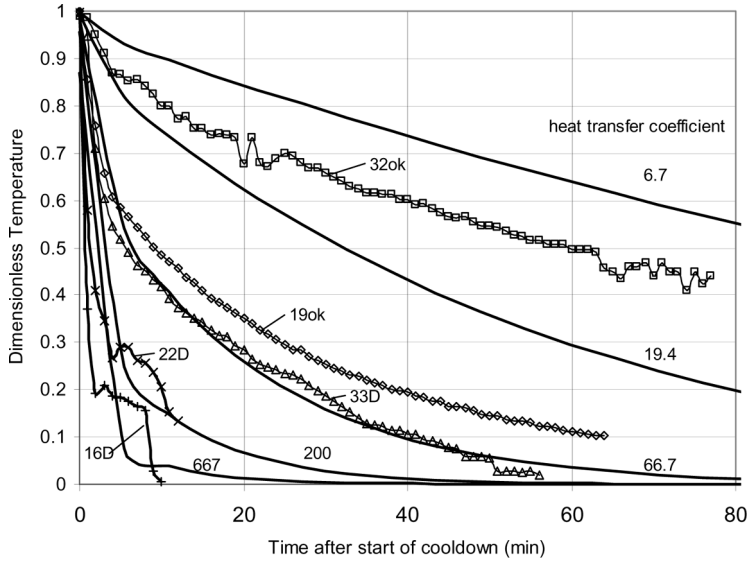

Figure 8. Experimental cooling rates for five tests.

reference plots in terms of the dimensionless temperature defined in Section II. The same reference graphs can be used to determine what the stress will be without having to make new computer runs. These graphs are shown in Fig. 8. Five of the tests have been plotted in this figure as well. The reference plots show the same results as found in Fig. 6, except they have been reduced to dimensionless-temperature form and, hence, cover the range of interest. Cooling rates slower than the slowest rate shown will not cause damage, and cooling rates faster than the fastest rate will.

The critical-damage cooling rate, which is determined in the following, decreases faster than those tests which showed survival and slower than those which showed damage. In order to estimate the critical-cooling rate, the critical stress is first obtained by determining the maximum stress in each test. This is done by first finding the corresponding heat-transfer coefficient for each test. The effective heat-transfer coefficient that each experiment corresponds to is obtained by first cross-plotting the dimensionless temperature from the reference plots versus h at a given time. An effective heat transfer coefficient can be estimated for each experiment, even those cooled in the furnace since the cylinder in that case is transferring heat from its surface to room temperature even though it is through the wall of the furnace. In Fig. 9, the dimensionless temperatures have been plotted versus h at two different times.

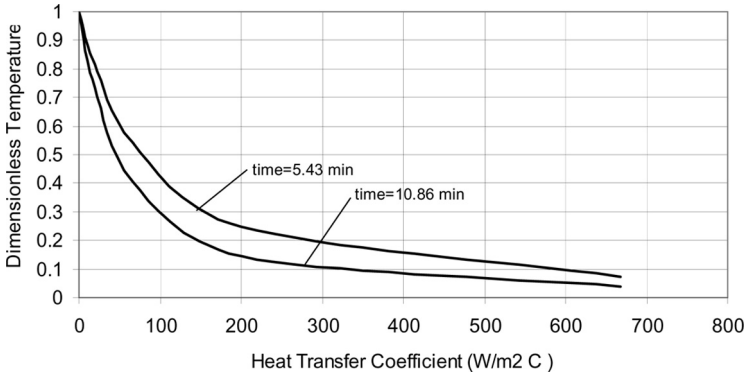

Figure 9. Dimensionless temperature versus heat transfer coefficient.

The dimensionless temperature from a given experiment at a given time was used to determine the value of h. For the five experiments in Fig. 8, the dimensionless temperatures at time = 10.86 minutes were picked from the graph. The later time was selected since that data is more accurate because, in all cases, the thermocouple was firmly reattached to the cylinder by that time. The values for h were then estimated from Fig. 9. These values are included in Table 2 for each of the five tests.

This analytical model assumes that the failure of a cylinder is related to the maximum thermal stress built up due to the transient temperature distribution. The maximum stress is then determined for each test with the heat-transfer coefficient of Table 2 as described in the following.

The maximum surface stress from Fig. 7 can be plotted versus heat-transfer coefficient for the five reference cases and are shown in Fig. 10. The heat-transfer coefficient determined in Table 2 can then be used in this figure to estimate the maximum stress for each of the tests. Since this plot applies to a 630°C hold temperature, it is necessary to adjust the results in each for the actual test temperature by the temperature ratio.

Table 2. Heat transfer coefficient for five tests

Test ID	Test 32ok	Test 33 D	Test 22 D	Test 19ok	Test 16D
Dimensionless temperature at t = 10.9 min	0.80	0.40	0.20	0.47	0.05
h (W/m^2C)	13.3	66.7	147	53.4	667

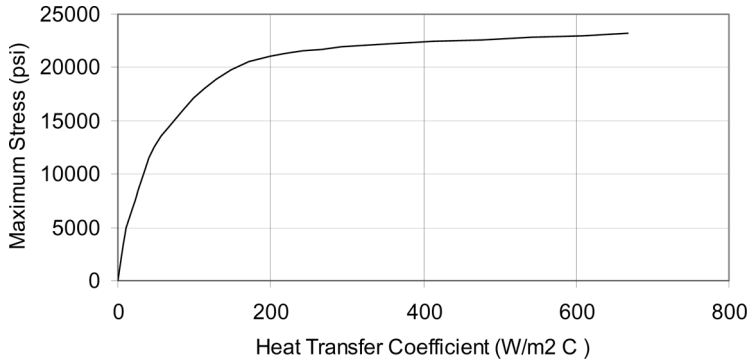

Figure 10. Maximum stress versus heat transfer coefficient for $T_{init} = 630°C$.

$$\sigma_{\max,T_{init}} = \sigma_{\max,630C} * \frac{(T_{init} - 25°C)}{(630°C - 25°C)} \tag{12}$$

Critical Stress Limit

Using the method presented above, the calculated stresses for the ten successful cylinder tests were obtained and are shown in Table 3. (Note: the data for the additional 5 tests are not included in Fig. 8, but are

Table 3. Calculated maximum stress

Test ID	H ($W/m^{2\circ}C$)	T_{init} (C)	σ_{max}(psi)
Test 16D	667	585	21,600
Test 22D	147	595	18,932
Test 33D	66.7	632	14,633
Test 40C	120	586	16,830
Test 50Cal*	107	587	16,569
Test 46C	80.0	588	14,175
Test 42C	53.3	608	12,783
Test 19ok	53.3	580	11,892
Test 32ok	13.3	635	4,901
Test 44ok	13.3	606	4,669

ok = undamaged in cool-down.
D = destroyed, many pieces.
C = cracked into 2 to 5 pieces.
*Cylinder center al rod.

plotted in Appendix A.) Table 3 results are grouped in order of decreasing damage from top to bottom. The test ID includes the result of the test, as well as the test number. As previously discussed, D stands for damaged (many pieces), C stands for cracked in 2 to 4 pieces, and ok means there was no visible damage. Correlating the maximum stresses with the cylinders that failed, Table 3 shows that cylinders that endured surface stresses of 12,700 psi and above failed, and those with stresses less than 12,000 psi did not.

The tensile-stress limit just determined is approximately 12,000 psi (17,000 psi if a 45 degree plane is considered), which is slightly greater than the 10,000 psi limit in the literature for glass. The calculated stress is proportional to CTE as is the tensile stress limit determined from these tests. As mentioned, a value of 9×10^{-6} cm/cm°C was used here. If a lower value were used, the stresses calculated would be lower, and so would the tensile stress limit determined from these experiments. So the tensile stress limit determined above must be used with the CTE used here. These are the values which will be used to estimate the critical-cooling rates for the large diameter CWFs to estimate if damage will occur with a given cooling rate. Since the calculated stress limit is proportional to the CTE used, it is the ratio of these two quantities which is the important limiting parameter.

Application to Production Consolidation Temperatures

The production consolidation temperature is 915°C. Stress during cool-down cannot start to build up until solidification occurs; therefore, damage to the cylinder could not occur until after the cylinder had cooled enough to solidify. Different sections, however, solidify at different times. The following is a very simple model: assume that the stress begins to build up when the surface temperature falls below 650°C, and that the maximum stress is calculated from the dimensionless stress at this temperature. This is a non-conservative approach and is not recommended. Instead (and until a more detailed model is available), the following conservative approach is recommended: calculate the maximum stress with the full temperature difference and use the 12,000 psi stress limit as the criteria for failure. Using this higher-calculated stress, one would conclude that damage occurs in some cases where it would not. But if the stress calculated with the full temperature difference is less than the 12,000 psi limit, a cylinder should not sustain damage during cool-down. However, as (5) points out, residual tensile stresses in the inner region can exist when the cylinder equilibrates at room temperature depending upon how fast it is cooled in the glass temperature transformation region.

Relation Between the Stress Limit and the Cooling Rate

The critical cooling rate can now be determined from the above determined stress limit. This is done for two different initial temperatures, 600°C and 915°C, using Fig. 10. The appropriate stress to use for each temperature is obtained by multiplying 12,000 psi by the temperature ratio as shown in Equation 13.

$$\sigma_{\max} = 12000 * \frac{(630^{\circ}C - 25^{\circ}C)}{(T_{init} - 25^{\circ}C)} \tag{13}$$

By calculating and using this maximum stress value with Fig. 10, the heat transfer coefficient correlated to the 12,000 psi limit is read from the graph. The values are 50.7 W/(m^2 °C) and 26.7 W/(m^2 °C) for T_{init} equal to 600°C and 915°C respectively. Model calculations were made for both of these h values and the results are included in Fig. 11, along with the other reference graphs.

Both of the added cooling-curve diagrams correspond to the maximum stress of 12,000 psi for different formation temperatures. Since our ultimate objective is to determine the cooling rates of the larger cylinders, we use these rates to estimate the cooling times of the large cylinders

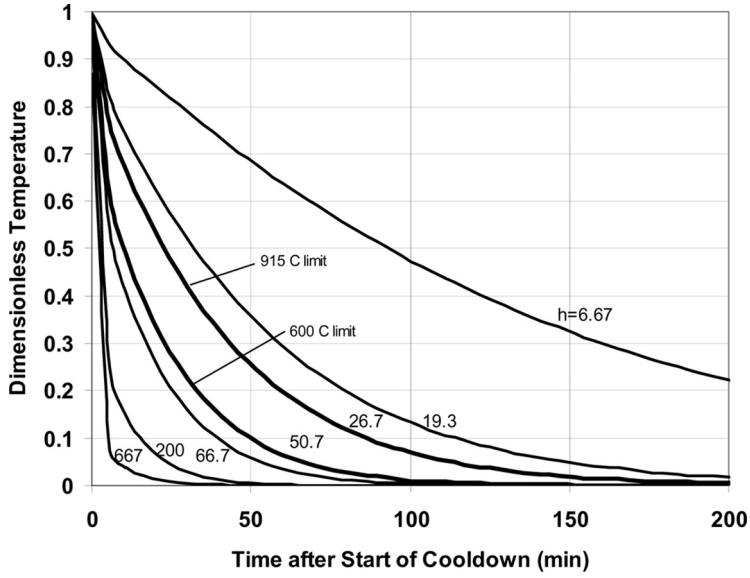

Figure 11. Critical cooling rates with two different initial temperatures for 7.8 cm cylinders.

to obtain the minimum cooling time applicable to the large size, which will be seen to be much longer than these small cylinders.

CONCLUSIONS: APPLICATION TO THE FULL SIZE CYLINDERS

Although the data obtained is for the glass component of the CWF only, it will be used to extrapolate a zeroth order estimate of the cooling time required to cool the large CWF cylinders. The critical cooling rate for 52- and 185-cm diameter glass cylinders can be estimated. It is realized that the actual composition of the CWF will affect these results, but still it is useful to have such an estimate to determine if the cooling time is a production problem requires further study and experimentation. The extrapolation is done by using the dimensional quantities of Section II to convert the values from the 915°C and 600°C curves in Fig. 11. The time required for any larger cylinder, cylinder 2, to reach the same dimensionless temperature as the 7.8 cm diameter cylinder, cylinder 1, is derived by equating dimensionless time defined in Equation 4 for the two cylinder which results in Equation 14.

$$t_2 = t_1 \times \frac{\alpha_1}{\alpha_2} \times \frac{R_2^2}{R_1^2} \tag{14}$$

For example, the time a 52-cm cylinder should take to cool-down to prevent stress cracking can be calculated. First, for a given value of h, the time after start of cool-down for a 7.8 cm diameter cylinder, t_1, is determined from Fig. 11 for any given dimensionless temperature. Next, this value is substituted in Equation 14 with the other known values and the time for a larger-diameter cylinder, t_2, is then computed for the same conditions. For the 3.9-cm diameter cylinders we experimented with, starting from an initial temperature 600°C, the surface can be cooled to 100°C in 42 minutes without cracking. Starting with an initial temperature of 915°C, the surface can be cooled to 100°C in 92 minutes without cracking. For a 52-cm diameter cylinder and an initial temperature 600°C, the surface can be cooled to 100°C in 31 hours without cracking or from 915°C to 100°C in 68 hours without cracking. The large 185-cm diameter cylinder, with an initial temperature of 600°C can be cooled to 100°C in 16 days without cracking or from 915°C, the surface can be cooled down to 100°C without damage in 36 days.

In order to cool the large diameter cylinders more slowly than the small diameter cylinders, the surface heat-transfer must be reduced for the large cylinders. The reduction can be calculated from the definition of the dimensionless heat-transfer coefficient (that is, the Nusselt

number) defined in equation 6. Equating the Nusselt number for two different cylinders results in Equation 15:

$$h_2 = h_1 \times \frac{R_1}{R_2} \times \frac{k_2}{k_1} \tag{15}$$

This equation implies a surprising but obvious conclusion. Consider the case where two cylinders of the same height, material, and temperature, but of different diameters, are set out to cool in air. Even when the smaller does not crack, the larger might because the free-convection heat-transfer coefficient is the same for both (due to their being the same height). The reason for this is that the surface temperature must be reduced more slowly for the larger diameter to keep the thermal stresses from building up to the stress limit.

In our production runs, the desired heat transfer will be accomplished with use of a cooling furnace. The above determined heat transfer coefficient will be used to determine the cooling rate that is required in the furnace.

Further experiments are planned to verify the above predicted R^2 effect of required cooling time with increasing diameter, assuming the larger diameters require so much additional cooling time. Methods of reducing the cooling time will be investigated as well. Also, since the production-consolidation temperatures are significantly higher (915°C) than those tested here (625°C), higher temperatures will be investigated. As mentioned previously, the stresses should not build up upon cool-down until solidification starts. Since solidification occurs in the region of 675°C to 625°C, the stresses at the higher consolidation temperature should not be much higher than in the 625°C consolidation tests.

REFERENCES

1. Bateman, K.J.; Solbrig, C.W., Benedict, R.W. (2006) Heat transfer design for ceramic waste forms from pyroprocessing, Proceedings of ICAPP '06, Reno, NV USA, June 4–8.
2. Bateman, K.J.; Solbrig, C.W. (2006) Using center hole heat transfer to reduce formation times for ceramic waste forms from pyroprocessing, Proceedings of 14th International Conference on Nuclear Engineering, ICONE, Miami, Florida 14-89794, July 17–20.
3. Frigo, A.A.; Wahlquist, D.R.; Willit, J.L. (2003) A conceptual advanced pyroprocess recycle facility, Global 2003 Topical ANS/ENS 2003 International. Winter Meeting, American Nuclear Society, New Orleans, Louisiana, November 16–20.
4. Battisti, T.J.; Goff, K.M.; Bateman, K.J.; Simpson, M.F.; Lind, J.P. (2002) Ceramic waste form production and development at ANL-West, American

Nuclear Society's Fifth Topical Meeting on Spent Nuclear Fuel and Fissile Materials Management, Charleston, SC, September 17–20.
5. Shand, E.B. (1958) *Glass Engineering Handbook*; McGraw-Hill Book Company: New York.
6. Solbrig, C.W. (2004) Plutonium sequestration with distributed nuclear islands, Proceedings of the Waste Management Symposium, Tucson, Arizona, Feb 29–Mar 4.
7. Lineberry, M.J.; Benedict, R.W.; Solbrig, C.W. (2004) Avoiding need for multiple repositories in a nuclear growth scenario, Proceedings of the Waste Management Symposium, Tucson, Arizona, Feb 29–Mar 4.
8. O'Holleran, T.P.; DiSanto, T.; Johnson, S.G. et al. (2000) Fracture toughness measurements on a glass bonded sodalite high-level waste form,Ceramic Transactions, **107**, (1999) in *Environmental Issues and Waste Management Technologies in the Ceramic and Nuclear Industries* V, G. T. Chandler and X. Feng, Ed.
9. Timoshenko, S.; Goodier, J.N. (1970) *Theory of Elasticity*, Third Ed., McGraw-Hill: New York.
10. Jaeger, J.C. (1945) On thermal stresses in circular cylinders, Philosophical Magazine, (36): 418-28.
11. Singh, J.P.; Thomas, Jr., J.R.; Hasselman, D.P.H. (1979) Analysis of effect of heat transfer variables on thermal stress resistance of brittle ceramics measured by quenching experiments, Thermal-Mechanical and Thermal Behavior of High-Temperature Structural Materials, Interim Report to Office of Naval Research, N00014-78-C-0431, Jan 1, December 31.
12. Ainsworth, J.A.; Herron, R.H. (1974) Thermal Shock Damage Resistance of Refractories, *J. Am. Ceramic. Soc.* (53): 533-38.
13. Manson, S.S.; Smith, R.W. (1956) Quantitative evaluation of thermal-shock resistance, Trans. of the ASME, (78): 533-544.
14. Curtis, C.E. (1947) Development of zirconia resistant to thermal shock, *J. Am. Ceram. Soc.*, (30): 180-196.
15. Carslaw, H.S.; Jaeger, J.C. (1959) *Conduction of Heat in Solids*; Oxford/Clarendon: London.
16. Callister, Jr., W.D. (1985). *Material Science and Engineering*; Wiley, Hoboken, New Jersey.
17. Hodgeman, C.D., Weast, R.C., Wallace, C.W. et al. (1954) *Handbook of Chemistry and Physics*; Chemical Rubber Publishing: Boca Raton, Louisiana.

APPENDIX A ADDITIONAL DATA

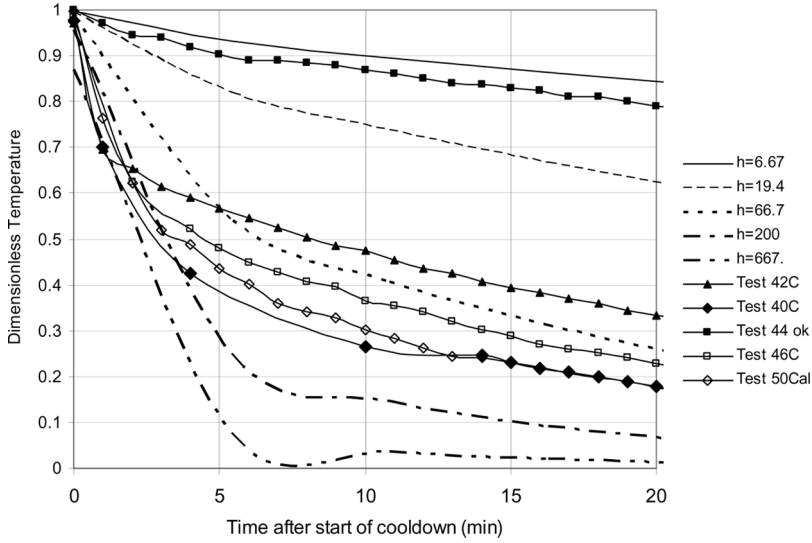

Figure A-1. Surface temperature profile of the five additional tests.